A Homogeneous Catalyst for Selective O_2 Oxidation at Ambient Temperature. Diversity-Based Discovery and Mechanistic Investigation of Thioether Oxidation by the $Au(III)Cl_2NO_3$(thioether)/O_2 System

Eric Boring, Yurii V. Geletii, and Craig L. Hill*

Contribution from the Department of Chemistry, Emory University, Atlanta, Georgia 30322

Received September 8, 2000

Abstract: A library of inorganic complexes with reversible redox chemistry and/or the ability to catalyze homogeneous oxidations by peroxides, including but not limited to combinations of polyoxometalate anions and redox-active cations, was constructed. Evaluation of library members for the ability to catalyze aerobic sulfoxidation (O_2 oxidation of the thioether, 2-chloroethyl ethyl sulfide, CEES) led to the discovery that a combination of $HAuCl_4$ and $AgNO_3$ forms a catalyst that is orders of magnitude faster than the previously most reactive such catalysts (Ru(II) and Ce(IV) complexes) and one effective at ambient temperature and 1 atm air or O_2. If no O_2 but high concentrations of thioether are present, the catalyst is inactivated by an irreversible formation of colloidal Au(0). However, this inactivation is minimal in the presence of O_2. The stoichiometry is $R_2S + {}^1/_2O_2 \rightarrow R_2S(O)$, a 100% atom efficient oxygenation, and not oxidative dehydrogenation. However, isotope labeling studies with $H_2{}^{18}O$ indicate that H_2O and not O_2 or H_2O_2 is the source of oxygen in the sulfoxide product; H_2O is consumed and subsequently regenerated in the mechanism. The rate law evaluated for every species present in solution, including the products, and other kinetics data, indicate that the dominant active catalyst is $Au(III)Cl_2NO_3$(thioether) (**1**); the rate-limiting step involves oxidation of the substrate thioether (CEES) by Au(III); reoxidation of the resulting Au(I) to Au(III) by O_2 is a fast subsequent step. The rate of sulfoxidation as Cl is replaced by Br, the solvent kinetic isotope effect ($k_{H_2O}/k_{D_2O} = 1.0$), and multiparameter fitting of the kinetic data establish that the mechanism of the rate-limiting step involves a bimolecular attack of CEES on a Au(III)-bound halide and it does not involve H_2O. The reaction is mildly inhibited by H_2O and the CEESO product because these molecules compete with those needed for turnover (Cl^-, NO_3^-) as ligands for the active Au(III). Kinetic studies using DMSO as a model for CEESO enabled inhibition by CEESO to be assessed.

Introduction

One of the ultimate challenges in catalysis is to formulate molecules or materials that catalyze useful (selective and reasonably rapid) reactions by O_2 or air under ambient conditions. Such catalysts would have a number of significant uses including the formulation of fabrics, coatings, and other materials that could catalytically clean the air and water by oxidative decontamination of the offending agents using solely the environment itself (air under ambient conditions). Unlike catalytic oxidation processes based on the second most economically and environmentally attractive oxidant, H_2O_2 (and related peroxides), there are almost no catalytic oxidation processes based on the most attractive oxidant, O_2/air, that proceed at a satisfactory rate at room temperature, thus certainly none that proceed rapidly, selectively, and without rapid catalyst decomposition under ambient conditions. Heterogeneous catalytic O_2-based oxidation processes typically are conducted between 270 and 720 °C (e.g., the O_2 oxidation of ethylene to ethylene oxide over Ag/Al_2O_3 is conducted at 270−290 °C and 30 bar O_2,[1] the oxidation of methanol to formaldehyde over 18−19 wt % Fe_2O_3 and 81−82 wt % MoO_3 is conducted at 350−450 °C with a large excess of O_2,[1] and the oxidation of isobutyric acid to methacrylic acid over polyoxometalates (POMs) is conducted at elevated temperatures and O_2 pressures).[2−5] The commercially important homogeneous catalytic O_2-based oxidations also all proceed well above ambient temperature. For example, the Mid-Century/Amoco process for oxidation of *p*-xylene to terephthalic acid catalyzed by cobalt and manganese acetates and bromides in acetic acid, the largest scale commercial homogeneous catalytic oxidation, is conducted at 225 °C using 15 atm O_2,[6,7] and the Wacker oxidation of ethylene to acetaldehyde catalyzed by $PdCl_2/CuCl_2$ is conducted at 120−130 °C using 4 atm O_2.[8]

Selectivity is a general problem in both stoichiometric and catalytic strictly O_2-based oxidations because these reactions are nearly always dominated by radical chain autoxidation, a chemistry that is intrinsically nonselective and difficult to

(1) Weissermel, K.; Arpe, H. J. *Industrial Organic Chemistry*, 3rd ed.; VCH: Weinheim, 1997.

(2) Ai, M.; Muneyama, E.; Kunishige, A.; Ohdan, K. *Bull. Chem. Soc. Jpn.* **1994**, *67*, 551−556.

(3) Misono, M. *Catal. Rev.-Sci. Eng.* **1987**, *29*, 269−321.

(4) Mizuno, N.; Misono, M. *Chem. Rev.* **1998**, *98*, 199−218.

(5) Marchal, C.; Davidson, A.; Thouvenot, R.; Hervé, G. *J. Chem. Soc., Faraday Trans.* **1993**, *89*, 3301−3306.

(6) Saffer, A.; Barker, R. S. Patent Publication (PCT), 58-US2833816.

(7) Partenheimer, W. *Catal. Today* **1995**, *23*, 69−158.

(8) Parshall, G. W.; Ittel, S. D. *Homogeneous Catalysis. The Applications and Chemistry of Catalysis by Soluble Transition Metal Complexes*, 2nd ed.; Wiley-Interscience: New York, 1992.

10.1021/ja0033133 CCC: $20.00
Published on Web 01/31/2001

control.[9−12] By "strictly" we mean that no reducing agent is present to convert O_2 to peroxo species or other forms of reduced oxygen that are both more reactive and more selective.[9] Nearly all enzyme-catalyzed oxidation processes, including some dioxygenase-catalyzed reactions, involve consumption of a reducing agent (most frequently NADH, NADPH, ascorbate, and thiols). The few cases that involve homogeneous catalytic oxidations strictly by O_2 are noteworthy, but none of these proceed effectively under ambient conditions (rates, selectivities, and stabilities that approach viable ranges).[10−15]

We report here the discovery of a Au(III)-based homogeneous catalyst for air (O_2)-based oxidations under ambient conditions that is significantly faster than any yet reported. We have chosen to probe this new catalyst using the O_2 oxidation of the thioether mustard analogue, 2-chloroethyl ethyl sulfide (CEES) to the corresponding sulfoxide, a reaction of current interest.[16−25] Heterogeneous oxidation catalysts based on Au are under considerable scrutiny at present. For $CO + {}^1/_2O_2 \rightarrow CO_2$ catalyzed by Au supported on TiO_2, the catalytic properties of Au depend on the support, the preparation method, and the size of the Au clusters. Optimal activity is achieved when the Au clusters are 3.0 nm in diameter, giving a turnover frequency (TOF) of 0.26 CO_2 (Au site)$^{-1}$ s^{-1}.[26] In solution, the stoichiometric oxidation of thioethers by Au(III) is well known, dating from 1901[27−32] to fairly thorough recent studies,[32−36] but there is only one report of catalytic oxidation by Au compounds. The oxidant in this case was nitrate not O_2.[37] Given the potential significance of a catalyst for selective and rapid oxidation by O_2 (or air) under ambient conditions, considerable effort has been expended to characterize this newly discovered Au-based catalyst despite its experimental sensitivity and complexity.

Experimental Section

Materials. $HAuCl_4$, $AgNO_3$, $AgClO_4$, $TBANO_3$, TBACl, $TBAHSO_4$, TMAOH, $TBAClO_4$, $TBABPh_4$ CH_3CO_2TBA, $TBAH_2PO_4$, anhydrous acetonitrile (CH_3CN), CEES, dimethyl sulfoxide (DMSO), 1,3-dichlorobenzene, and 95% labeled $H_2{}^{18}O$ were purchased from Aldrich. $TBANO_2$ was purchased from Fluka (TBA and TMA are abbreviations for tetra-*n*-butylammonium and tetramethylammonium cations, respectively). Diethyl ether and acetone were purchased from Aldrich and filtered through a column of neutral alumina before use. All POMs in the library (Figure 1) were synthesized from literature preparations.[38−62] All reagents except for $H_2{}^{18}O$ (Aldrich) were dried in vacuo overnight. Stock solutions were prepared using anhydrous CH_3CN.

General Procedures. All gas chromatography analyses were performed on an HP5890 gas chromatograph equipped with a FID detector and a 5% phenyl methyl silicone capillary column. Mass abundance determinations were performed using a HP 5890 GC with a 5% phenyl methyl silicone capillary column and a 5971A mass selective detector. UV−visible spectra were run on a HP 8452A diode array spectrophotometer. The percentages of O_2 in or comprising the reaction atmosphere were varied using a series 810 Mass Trak flowmeter with dried argon as the other gas.

(9) Sheldon, R. A.; Kochi, J. K. *Metal-Catalyzed Oxidations of Organic Compounds*; Academic Press: New York, 1981.
(10) Neumann, R.; Dahan, M. *Nature* **1997**, *388*, 353−355.
(11) Hill, C. L.; Weinstock, I. A. *Nature* **1997**, *388*, 332−333.
(12) Hill, C. L. *Nature* **1999**, *401*, 436−437.
(13) Groves, J. T.; Quinn, R. *J. Am. Chem. Soc.* **1985**, *107*, 5790−5792.
(14) Neumann, R.; Dahan, M. *J. Am. Chem. Soc.* **1998**, *120*, 11969−11976.
(15) Weiner, H.; Finke, R. G. *J. Am. Chem. Soc.* **1999**, *121*, 9831−9842.
(16) Chambers, R. C.; Hill, C. L. *J. Am. Chem. Soc.* **1990**, *112*, 8427−8433.
(17) Yang, Y. C.; Baker, J. A.; Ward, J. R. *Chem. Rev.* **1992**, *92*, 1729−1743.
(18) Sattari, D.; Hill, C. L. *J. Am. Chem. Soc.* **1993**, *115*, 4649−4657.
(19) Gall, R. D.; Faraj, M.; Hill, C. L. *Inorg. Chem.* **1994**, *33*, 5015−21.
(20) Gall, R. D.; Hill, C. L.; Walker, J. E. *Chem. Mater.* **1996**, *8*, 2523−2527.
(21) Gall, R. D.; Hill, C. L.; Walker, J. E. *J. Catal.* **1996**, *159*, 473−478.
(22) Hill, C. L.; Gall, R. D. *J. Mol. Catal. A: Chem.* **1996**, *114*, 103−111.
(23) Menger, F. M.; Elrington, A. R. *J. Am. Chem. Soc.* **1990**, *112*, 8201−8203.
(24) Yang, Y.; Szafraniec, L. L.; Beaudry, W. T.; Davis, F. A. *J. Org. Chem.* **1990**, *55*, 3664−3666.
(25) Hay, R. W.; Clifford, T.; Govan, N. *Transition Met. Chem.* **1998**, *23*, 619−624.
(26) Valden, M.; Lai, X.; Goodman, D. W. *Science* **1998**, *281*, 1647−1650. See also a recent general reference on basic and applied Au chemistry: Schmidbauer, H. *Gold: Chemistry, Biochemistry and Technology*; Wiley-Interscience: New York, 1999.
(27) Phillips, F. C. *J. Am. Chem. Soc.* **1901**, *23*, 257.
(28) Hermann, F. *Ber. Dtsch. Chem. Ges.* **1905**, *28*, 2813.
(29) Brain, F. H.; Gibson, C. S.; Jarvis, J. A. J.; Phillips, R. F.; Powell, H. M.; Tyabii, A. *J. Chem. Soc.* **1952**, 3686.
(30) Puddephatt, R. J. In *Comprehensive Coordination Chemistry: The Synthesis, Reactions, Properties, and Applications of Coordination Compounds*, 1 ed.; Wilkinson, G., Gillard, R. D., McCleverty, J. A., Eds.; Pergamon Press: Oxford, 1987; Vol. 5.
(31) Elding, L. I.; Olsson, L. F. *Inorg. Chem.* **1982**, *21*, 779−784.
(32) Elding, L. I.; Skibsted, L. H. *Inorg. Chem.* **1986**, *25*, 4084−4087.
(33) Berglund, J.; Elding, L. I. *Inorg. Chem.* **1995**, *34*, 513−519.
(34) Elmroth, S.; Elding, L. I. *Inorg. Chem.* **1996**, *35*, 2337−2342.
(35) Ericson, A.; Elding, L. I.; Elmroth, S. K. C. *J. Chem. Soc., Dalton Trans.* **1997**, *7*, 1159−1164.
(36) Annibale, G.; Canovese, L.; Cattalini, L.; Natile, G. *J. Chem. Soc., Dalton Trans.* **1980**, 1017−1021.
(37) Gasparrini, F.; Giovannoli, M.; Misiti, D.; Natile, G.; Palmieri, G. *Tetrahedron* **1983**, *39*, 3181−3184.
(38) Maksimov, G. M.; Kustova, G. N.; Matveev, K. I.; Lazarenko, T. P. *Koord. Khim.* **1989**, *15*, 788−96.
(39) O'Donnell, S. E.; Pope, M. T. *J. Chem. Soc., Dalton Trans.* **1976**, 2290−7.
(40) Pope, M. T. *Inorg. Chem.* **1972**, *11*, 1973.
(41) Pope, M. T.; O'Donnell, S. E.; Prados, R. A. *Chem. Commun.* **1975**, 22−23.
(42) Yurchenko, E. N. *J. Mol. Struct.* **1980**, *60*, 325−31.
(43) Bazhenova, T. A.; Ioffe, M. S.; Kachapina, L. M.; Lobkovskaya, R. M.; Shibaeva, R. P.; Shilov, A. E.; Shilova, A. K. *Zh. Strukt. Khim.* **1978**, *19*, 1047−62.
(44) Tourné, C.; Tourné, G. *Bull. Soc. Chim. Fr.* **1969**, *4*, 1124−36.
(45) Marcu, G.; Patrut, A.; Botar, A. *Rev. Chim. (Bucharest)* **1989**, *40*, 870−875.
(46) Kuznetsova, N. I.; Kuznetsova, L. I.; Detusheva, L. G.; Likholobov, V. A.; Fedotov, M. A.; Koscheev, S. V.; Burgina, E. B. *Stud. Surf. Sci. Catal.* **1997**, *110*, 1203−1211.
(47) Hamlaoui, M. L.; Vlassenko, K.; Messadi, D. *C. R. 'Acad. Sci., Ser. II* **1990**, *311*, 795−798.
(48) Huang, R. D.; Bei, B. L.; Wang, E. B.; Li, B. T.; Zhang, S. X. *Gaodeng Xuexiao Huaxue Xuebao* **1998**, *19*, 1721−1723.
(49) Tézé, A.; Souchay, P. C. R. *C. R. Acad. Sci., Ser. C* **1973**, *276*, 1525−1528.
(50) Tsyganok, L. P.; Statsenko, V. P.; Vil'dt, A. L. *Zh. Neorg. Khim.* **1974**, *19*, 3071−3077.
(51) Nomiya, K.; Kobayashi, R.; Miwa, M. *Polyhedron* **1985**, *4*, 149.
(52) Preuss, F.; Rosenhahn, L. *J. Inorg. Nucl. Chem.* **1972**, *34*, 1691−1703.
(53) Gong, J.; Li, G.; Wang, F.; Qu, L. *Wuji Huaxue Xuebao* **1995**, *11*, 232−237.
(54) Varga, J., G. M.; Papaconstantinou, E.; Pope, M. T. *Inorg. Chem.* **1970**, *9*, 662.
(55) Tret'yakov, V. P. *Kinet. Katal.* **1993**, *34*, 227−9.
(56) Weakley, T. J. R.; Finke, R. G. *Inorg. Chem.* **1990**, *29*, 1235−1241.
(57) Liu, H.; Sun, W.; Yue, B.; Li, M.; Chen, Z.; Jin, S.; Xie, G.; Shao, Q.; Wu, T.; Chen, S.; Yan, X. *Wuji Huaxue Xuebao* **1997**, *13*, 251−257.
(58) Lyon, D. K.; Miller, W. K.; Novet, T.; Domaille, P. J.; Evitt, E.; Johnson, D. C.; Finke, R. G. *J. Am. Chem. Soc.* **1991**, *113*, 7209−7221.
(59) Evans, H. T.; Tourné, C. M.; Tourné, G. F.; Weakley, T. J. R. *J. Chem. Soc., Dalton Trans.* **1986**, 2699−2705.
(60) Gómez-García, C. J.; Coronado, E.; Gómez-Romero, P.; Casañ-Pastor, N. *Inorg. Chem.* **1993**, *32*, 3378−3381.
(61) Gómez-García, C. J.; Coronado, E.; Ouahab, L. *Angew. Chem., Int. Ed. Engl.* **1992**, *31*, 649−651.
(62) Gómez-García, C. J.; Borrás-Almenar, J. J.; Coronado, E.; Ouahab, L. *Inorg. Chem.* **1994**, *33*, 4016−4022.

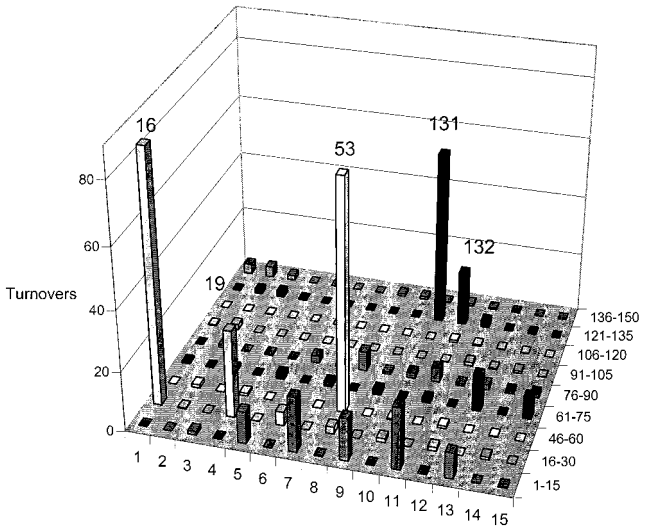

Figure 1. Combinatorial library of catalysts for the oxidation of CEES. Catalytic activity (turnovers of CEESO after 11 h) is depicted on the *z* axis. Each entry on the *x*,*y* plane (base plane) represents a distinct catalyst. Formulas of all the entries (primarily POM derivatives) are given in the Supporting Information (Table S1). Catalytic activity was assessed in an identical manner for all 150 members of the library (see text for details). Catalyst 131 was the Au/Ag/NO_3^- combination (in less than ideal mole ratios) that led to discovery of the parent system (optimized mole ratios) that was subsequently investigated in depth.

Evaluation of the Library of Catalysts. A total of 150 combinations of substituted POM anions and countercations were generated, and each was evaluated for the ability to catalyze the oxidation of CEES by O_2 (see Figure 1). For the 150 reactions, every other reaction involved mixing 1.0 equiv of a POM with 5 equiv of $HAuCl_4$ in a 20-mL vial. The other vials contained POM only. A few vials contained POM-free control compounds. The compositions of all entries in the library are summarized in Table S1 in the Supporting Information. Each vial was purged with O_2, and 1.0 mL of a solution containing 100 equiv of CEES and 50 equiv of 1,3-dichlorobenzene, the internal standard for gas chromatographic analysis, in CH_3CN was added via syringe. Each reaction was monitored at 4 and 11 h for turnovers of CEESO. Product distributions were quantified by GC.

General Procedure for Sample Preparation. Stock solutions of $HAuCl_4$, $AgNO_3$, $AgClO_4$, $TBANO_3$, TBACl, and $TBAClO_4$ were prepared in anhydrous CH_3CN and wrapped with aluminum foil to prevent light exposure. All reagents were dried in vacuo before they were dissolved in anhydrous CH_3CN. Appropriate amounts of each stock solution were added via syringe to a 20-mL glass vial fitted with a PTFE septum that was first purged with O_2. (The precise amounts of all reactants and other reagents and conditions are given in the figure captions.) The atmospheric pressure was adjusted to 1.0 atm by inserting a needle into the septum for several seconds. The reactions were carried out at 25 ± 1 °C.

Analysis of Precipitate Formed after CEES Addition. In a 20-mL vial purged with O_2, 0.10 mL (4.8×10^{-6} mol, 1 equiv) of $HAuCl_4$, 0.035 mL (3.6×10^{-6} mol, 0.75 equiv) of $AgNO_3$, 0.06 mL (6.0×10^{-6} mol, 1.25 equiv) of $AgClO_4$, and 0.083 mL (7.2×10^{-4} mol, 150 equiv) of 1,3-dichlorobenzene were added by syringe. The volume was adjusted to 0.96 mL with anhydrous CH_3CN. After the solution was stirred for 1 min, 0.042 mL of CEES (3.6×10^{-4} mol, 75 equiv) was added and the solution was allowed to stir for an additional 1 min. The vial was then centrifuged and the solution was filtered off leaving a white precipitate. The precipitate was washed with a small amount of CH_3CN and dried under reduced pressure overnight. Elemental analyses confirmed the precipitate was AgCl. Anal. Calcd for AgCl: Ag, 75.26; Cl, 24.74. Found: C, 0.03; H, 0.08; N, 0.03; Ag, 75.08; Cl, 24.89.

Substituting NO_3^- with Other Anions. These experiments were conducted using protocols and solutions similar to those in the experiments described above. Solutions of 0.095 mL (9.5×10^{-6} mol, 2 equiv) of $AgClO_4$, 0.10 mL (4.8×10^{-6} mol, 1 equiv) of $HAuCl_4$, and 0.083 mL (7.2×10^{-4} mol, 150 equiv) of 1,3-dichlorobenzene were added by syringe to a 20-mL vial that was purged with O_2. Solutions of the following in anhydrous CH_3CN (all 0.2 M) were prepared in 20-mL vials: $TBANO_2$, $TBABPh_4$, $TBAHSO_4$, TMAOH, $TBAPF_6$, CH_3CO_2TBA, and $TBAH_2PO_4$. Each of the aforementioned 0.2 M solutions (0.024 mL, 4.8×10^{-6} mol, 1 equiv) was added to vials containing the Au/Ag solution. The volume was adjusted to 0.96 mL with anhydrous CH_3CN. After stirring for 1 min, 0.042 mL of CEES was added by syringe. Aliquots were analyzed by GC every 15 min.

Assessment of Au(III) Concentration. For a blank, CH_3CN (2.00 mL) was added to a 1.0-cm quartz cuvette equipped with a stopcock sidearm, a standard taper 14/20 joint, a magnetic stirring bar, and a septum stopper. The background absorbance of this blank was measured on a HP 8452A diode array spectrophotometer. To this cuvette was added by syringe stock solutions of 0.089 mL (9.0×10^{-6} mol, 0.75 equiv) of $AgNO_3$, 0.15 mL (1.5×10^{-5} mol, 1.25 equiv) of $AgClO_4$, and 0.12 mL (1.2×10^{-6} mol , 1.0 equiv) of $HAuCl_4$. It was apparent from the spectrum of this solution, that the 350−450-nm range was the optimal wavelength for quantifying the concentration of Au(III). The solution was immediately transferred to a 20-mL vial that was purged with either 100% O_2 or a mixture of 50:50 O_2 and Ar. To this solution was added 0.020−0.155 mL (3.5×10^{-4} mol, 30 equiv) of CEES. After shaking for 1 min, the vial was centrifuged and the solution was transferred back to the cuvette previously purged with O_2 and spectra were collected during the reaction time every 5−10 min. Every 15 min, CEES consumption and CEESO formation were quantified by analyzing 1-μL aliquots by GC.

Establishing the Stoichiometry with Respect to O_2. O_2 consumption was determined by a volummetric method. The reaction vessel containing 1.36 mL of CH_3CN was purged by O_2, and solutions (all in CH_3CN) of 0.20 mL (5.0×10^{-6} mol) of $HAuCl_4$, 0.094 mL (5.0×10^{-6} mol) of $AgNO_3$, 0.094 mL (5.0×10^{-6} mol) of $AgClO_4$, and 0.166 mL (7.5×10^{-4} mol) of 1,3-dichlorobenzene (internal standard for GC) were added via syringe through a rubber septum stopper. The reaction was initiated by injection of 0.084 mL (3.8×10^{-4} mol) of CEES. The consumption of O_2 was recorded, and 1-μL aliquots were periodically taken and injected into the GC to quantify CEESO formation.

Evaluation of the Reaction Kinetics. The kinetic data were evaluated and curves fit using the Solver subprogram of the Microsoft Excel. The sums of the squares of the difference between experimental and theoretical values were minimized. When fitting was performed varying two parameters at once, several minimums were found in some cases. In this event, the parameters giving the least deviation from experimental data were used.

Rate Law Determination for CEES Oxidation by O_2 Catalyzed by the $HAuCl_4/AgNO_3/AgClO_4$ System. Screening of a library followed by subsequent evaluation of various Ag(I) salt mixtures identified the most reactive O_2-based catalyst as one composed of $AgNO_3$, $AgClO_4$, and $HAuCl_4$; thus this system was chosen for further investigation. When 1.0 equiv of $HAuCl_4$ was used, the optimal reactivity was achieved with 0.75 and 1.25 equiv of Ag(I) and NO_3^- respectively. The order of each component was determined by varying its concentration over the range given below while the concentrations of all other components were held constant. Unless otherwise noted, the initial concentration of $HAuCl_4$, $[HAuCl_4]_o$, used in each reaction was 4.8 mM. $[CEES]_o$ was varied from 0.15 to 3.1 M. $[Ag(I)]_o$ was varied from 0 to 15.2 mM, $[HAuCl_4]_o$ was varied from 0 to 11.9 mM, and $[NO_3^-]_o$ was varied from 0 to 54 mM. To establish the order in the active multicomponent catalyst itself, the following ratio of concentrations of catalyst components [2Ag(I)/1Au(III)/0.75NO_3^-] was varied from 1.2 to 7.4 mM (based on total Au concentration). $[Cl^-]_o$ was varied from 0 to 6.3 mM, and $[ClO_4^-]_o$ was varied from 0 to 0.1 M. The kinetic impact of the product sulfoxide was assessed using DMSO as a model for CEESO (CEESO itself could not, of course, be used because it is the actual product). $[DMSO]_o$ was varied from 0 to 0.36 M, $[H_2O]_o$ was varied from 0 to 0.91 M, and the percentage of O_2 in the gas phase (headspace over reaction) was varied from 0 to 100%. For rate order determinations, initial rate methods were employed as

per convention. Given the lack of reactivity of the CEESO product under the reaction conditions, the reactions were monitored until at least 10% of the starting CEES had been consumed.

$H_2{}^{18}O$ Labeling Experiment. To determine the atomic origin of oxygen in the sulfoxide product (H_2O, H_2O_2, or O_2), an experiment using $H_2{}^{18}O$ was performed. For this experiment, a stock solution of 1.53 M $H_2{}^{18}O$ in anhydrous CH_3CN was prepared using 95 atom % ^{18}O-labeled H_2O. All other stock solutions used were the same as those in the previous experiments. In a 20-mL vial purged with O_2, 0.10 mL (4.8×10^{-6} mol, 1 equiv) of $HAuCl_4$, 0.035 mL (3.6×10^{-6} mol, 0.75 equiv) of $AgNO_3$, 0.06 mL (6.0×10^{-6} mol, 1.25 equiv) of $AgClO_4$, and 0.083 mL (7.2×10^{-4} mol, 150 equiv) of 1,3-dichlorobenzene internal standard were added by syringe. The volume was adjusted to 0.82 mL with anhydrous CH_3CN. After the solution was stirred for 1 min, 0.042 mL of CEES (3.6×10^{-4} mol, 75 equiv) was added followed immediately by 0.140 mL of $H_2{}^{18}O$ (3.6×10^{-4} mol, 75 equiv). The isotopic composition of the products was quantified by GC/MS.

Assessment of H_2O_2-Based Sulfoxidation. To assess sulfoxidation arising from any H_2O_2 generated in situ, an experiment using H_2O_2 was performed. In a Schlenk flask, 2.0 mL of a 30% aqueous H_2O_2 solution was reduced in volume to 0.7 mL resulting in 85% v/v H_2O_2. *Caution. The procedure of concentrating H_2O_2 or any other peroxide is potentially dangerous. There is some risk of explosion.* The concentrated H_2O_2 solution was immediately diluted with anhydrous CH_3CN and titrated iodometrically; final $[H_2O_2] = 1.2$ M in CH_3CN. The same concentrations of each component were used as in the $H_2{}^{18}O$ experiment except that the $H_2{}^{18}O$ was omitted. After allowing the solution to react for 2 h, 0.060 mL of the 1.2 M H_2O_2 solution (7.2×10^{-5} mol, 15.0 equiv) was added by syringe.

Solvent Kinetic Isotope Effect, k_{H_2O}/k_{D_2O}. In a 20-mL vial purged with O_2, 0.10 mL (4.8×10^{-6} mol, 1 equiv) of $HAuCl_4$, 0.035 mL (3.6×10^{-6} mol, 0.75 equiv) of $AgNO_3$, 0.060 mL (6.0×10^{-6} mol, 1.25 equiv) of $AgClO_4$, and 0.083 mL (7.2×10^{-4} mol, 150 equiv) of 1,3-dichlorobenzene were added by syringe. The volume was adjusted with 0.675 mL of anhydrous CH_3CN. To this solution were added, 0.042 mL (3.6×10^{-4} mol, 75 equiv) of CEES, immediately followed by 0.0065 mL (3.6×10^{-4} mol, 75 equiv) of D_2O. In a separate experiment, the same procedure was used except that H_2O was substituted for D_2O. The rate behaviors for the two systems (H_2O and D_2O) were compared.

Replacement of Cl^- Ligands with Br^- Ligands To Assess Atom Transfer in Rate-Limiting Step. In a 20-mL vial purged with O_2, 0.10 mL (4.8×10^{-6} mol, 1 equiv) of $HAuBr_4$, 0.035 mL (3.6×10^{-6} mol, 0.75 equiv) of $AgNO_3$, 0.060 mL (6.0×10^{-6} mol, 1.25 equiv) of $AgClO_4$, and 0.083 mL (7.2×10^{-4} mol, 150 equiv) of 1,3-dichlorobenzene were added by syringe. The volume was adjusted to 0.680 mL with anhydrous CH_3CN. To this solution, 0.041 mL of CEES (3.5×10^{-4} mol, 75 equiv) was added by syringe. The reaction products were quantified as a function of time by GC and GC/MS as described above. Another experiment was performed using the same procedure except that the volume was adjusted to 0.315 mL with CH_3CN and 0.406 mL of CEES was used.

Attempted Oxidation of Dimethyl Sulfoxide to Dimethyl Sulfone. In a 20-mL vial purged with O_2, 0.10 mL (4.8×10^{-6} mol, 1 equiv) of $HAuCl_4$, 0.035 mL (3.6×10^{-6} mol, 0.75 equiv) of $AgNO_3$, 0.060 mL (6.0×10^{-6} mol, 1.25 equiv) of $AgClO_4$, and 0.083 mL (7.2×10^{-4} mol, 150 equiv) of 1,3-dichlorobenzene were added by syringe. The volume was adjusted to 0.820 mL with anhydrous CH_3CN. To this solution, 0.025 mL (3.6×10^{-4} mol, 75 equiv) of DMSO was added by syringe. The reaction products were quantified as a function of time by GC and GC/MS as described above.

Effect of DMSO (a CEESO Model) on the Rate. In a 20-mL vial purged with O_2, 0.100 mL (4.77×10^{-6} mol, 1 equiv) of $HAuCl_4$, 0.035 mL (3.58×10^{-6} mol, 0.75 equiv) of $AgNO_3$, 0.060 mL (5.96×10^{-6} mol, 1.25 equiv) of $AgClO_4$, and 0.083 mL (7.15×10^{-4} mol, 150 equiv) of 1,3-dichlorobenzene were added by syringe. The total volume, factoring in for added CEES and DMSO, was adjusted to 1.0 mL with anhydrous CH_3CN. To the vial, 0.045 mL (3.58×10^{-4} mol, 75 equiv) of CEES was added immediately followed by DMSO. The concentration of added DMSO was varied from 0 to 0.36 M.

Results

Identification of Au(III)Cl_2NO_3(thioether)/O_2 Catalytic Oxidation System. A 150-member library was constructed, largely but not exclusively, by combining polyoxoanions (POMs for convenience) and selected cations. Each member of this library was evaluated for its ability to catalyze oxidation of the thioether (CEES) using only O_2 as the oxidant under ambient conditions (room temperature and atmospheric pressure). The POMs chosen were largely those known to have reversible redox chemistry and/or the ability to catalyze homogeneous oxidations by peroxides and other terminal oxidants under mild conditions. The cations chosen included redox-active d-block ions or their precursors including $HAuCl_4$ as well as the s-block and p-block (e.g., quaternary ammonium) cations conventionally used as the counterions in POMs. This library also contained POM-free control formulations such as the chloride, nitrate, or perchlorate salts of the same redox-active d-block cations used in combination with the POMs. Figure 1 (Experimental Section) summarizes the results of one such library (all members of this library on the *x*,*y*-base plane are given in Table S1 in the Supporting Information). While most showed little or no activity, three (entries 16, 53, and 131) exhibited considerable activity. The compositions of these three catalysts were $CuPW_{11}O_{39}^{5-}$, $MnPW_{11}O_{39}^{5-}$, and $AgNO_3$, each with 5 equiv of $HAuCl_4$. The rate of the third or POM-free system based on Au and Ag was increased severalfold by varying the ratios of $HAuCl_4$ and $AgNO_3$ (and subsequently the ratios of different Ag(I) salts) such that it became the fastest catalyst we evaluated and significantly faster than the two most reactive catalysts in the literature for the homogeneous O_2-based oxidation of thioethers, $RuCl_2(Me_2SO)_4$,[63] and $(NH_4)_2Ce(NO_3)_6$.[64] The former catalyst produces 3.4 turnovers h^{-1} of tetrahydrothiophene oxide (THTO) from tetrahydrothiophene (THT) at 110 °C and 110 psig of O_2, while the latter catalyst produces 17.6 turnovers of THTO from THT after 30 min at 60 °C and 14 bar O_2. *Neither $RuCl_2(Me_2SO)_4$ nor $(NH_4)_2Ce(NO_3)_6$ has demonstrable activity at ambient temperature*. The *unoptimized* Au(III)/Ag(I) system arising from the library in Figure 1 was producing nearly comparable turnovers to the Ce(IV) system, the more reactive of the two literature catalysts, at ambient temperature and only 1 atm O_2. Specifically, this initial system ($1AgNO_3/5HAuCl_4$ only) gave 35.4 turnovers of CEESO after 4 h under these very mild conditions. Furthermore, CEES is significantly harder to oxidize than THT both thermodynamically and kinetically (it is less reducing and less nucleophilic).[19] Given the remarkable reactivity of this mixture of Au(III) and Ag(I) salts, we chose to investigate this new catalyst in detail. The principal system used in this study comprises 1, 0.75, and 1.25 equiv of the $HAuCl_4$, $AgNO_3$, and $AgClO_4$ precursors respectively, based on rate and tractability (ability to vary the concentrations of other added species and maintain completely homogeneous reaction conditions at all times). We report here the general features of this catalytic system, the thioether oxidation reaction stoichiometry, the complex rate law and other kinetic features of this reaction, and the reaction mechanism.

General Features of the Au(III)Cl_2NO_3(thioether)/O_2 Catalytic Oxidation System. Extensive studies of *stoichiometric* thioether oxidation by Au(III) complexes in the literature have established five points: (1) $HAuCl_4$ does not oxidize thioethers at a measurable rate under ambient conditions; (2) halide and thioether ligands exchange in rapid preequilibria

(63) Riley, D. P. *Inorg. Chem.* **1983**, *22*, 1965−1967.
(64) Riley, D. P.; Smith, M. R.; Correa, P. E. *J. Am. Chem. Soc.* **1988**, *110*, 177−180.

before the rate-limiting redox step that involves thioether reduction of Au(III) forming Au(I) and sulfoxide; (3) the formation constant for the Au(III) complex with one thioether ligand (K_1) is greater than the formation constant for the Au(III) complex with two thioether ligands (K_2); (4) Au(III) complexes with three thioether ligands do not form (K_3 is too small to measure); and (5) the lability of the transient Au(III) complexes renders them nonisolable.[35−37,65,66] The data given below indicate our Au(III)-based catalytic system for O_2 oxidation shares these features of the stoichiometric thioether−Au(III) studies. However, the catalytic system has additional components and is more mechanistically complex.

Like the Au catalyst precursor, $HAuCl_4$, by itself, and the Ag salt precursors, $AgNO_3$ and $AgClO_4$, by themselves, are both effectively inactive as catalysts for the air oxidation of thioethers at ambient temperature and pressure ($HAuCl_4$ and $AgNO_3$ are entries 1 and 130 in the library, Figure 1, respectively). The addition of a soluble Ag(I) salt (e.g., $AgNO_3$ or $AgClO_4$) to $AuCl_4^-$ does not result in the immediate precipitation of AgCl. However, the addition of CEES to the Au(III)/Ag(I) solution leads to the immediate disappearance of the yellow chromophore of Au(III) and the precipitation of AgCl (confirmed by elemental analysis after isolation). Quantification of CEES consumption and CEESO generation confirmed the stoichiometry in eq 1 for this catalyst preparation reaction.

$$AuCl_4^- + 2CEES + 2Ag^+ + H_2O \rightarrow AuCl(CEES) + CEESO + HCl + H^+ + 2AgCl \quad (1)$$

Analysis of the soluble catalyst after removal of AgCl (by taking the reaction to dryness) indicated it contained Au and CEES and/or CEESO moieties but no Ag. Attempted recrystallization of this material produced only a catalytically inactive powder that analyzed for Au(0): Au, 99.83; H, 0.08; C, 0.02. If the catalyst is prepared using 5 mM Au, and excess CEES in the absence of O_2, the resulting Au(0) colloid is violet, suggesting the Au(0) clusters are ∼80−100 nm. The attempted growth of crystals of the active catalyst involved much higher concentrations of Au and diffusion of ether into the CH_3CN solution. This procedure produced a colloid that was gold in color consistent with the presence of particles of <40 nm in diameter. (Au(0) colloids are blue/violet, red, or brown/gold for average particle sizes of 80−100, 40−80, and <40 nm, respectively.)[67] The likely concentrations of the Au(0) particles present during colloid formation are consistent with the different particle sizes and colors.[68]

Once Au(0) forms in this system, it is not reoxidized, and thus this represents an irreversible inactivation of the catalyst. However, use of the ratios of reactants in the following experiments and in the presence of O_2, or even ambient air, produces soluble Au-based catalysts that remain in solution and retain activity for at least one week.[69]

This catalyzed aerobic thioether (CEES) oxidation exhibits a short induction phase followed by the main reaction. This is illustrated in Figure 2. Control experiments establish that the byproducts (not shown) vinyl chloride and thioformaldehyde hydrate result exclusively from thermal decomposition of the CEESO product in the hot injector port of the gas chromatograph. When correction is made for this (or it is eliminated completely by using lower injector port temperatures), the selectivity for sulfoxide is 97 ± 5%. This minimum error is dictated by the limits of the FID detector of the GC. While it is the main reaction itself and not the induction period that is of principal importance and interest, it is appropriate to examine the induction period because it sometimes provides information about the main reaction and because it formally constitutes a component of the overall reaction. After reduction of the starting Au(III) complex, eq 1, the system remains colorless and catalytically inactive during an induction period. During the induction period, no CEES is consumed and no CEESO is formed (Figure 2). At the end of the induction period, the solution rapidly becomes yellow, and the electronic absorption spectrum (350−450 nm) is very similar to that of conventional isolable square-planar Au(III) complexes.[70] During the main reaction (after the induction period), the concentration of Au(III) remains constant, CEES is consumed, and CEESO is formed (Figure 2, including inset). The dotted and solid lines in Figure 2 arise from fitting of experimental data to the proposed mechanism and are addressed in the Discussion section. While it may not be readily apparent from Figure 2, the kinetics of CEES consumption and CEESO formation in the main reaction do not obey any simple kinetic law; the reaction gradually slows down as a result of a mild inhibition by CEESO product (vide infra). The length of the induction period depends on concentrations of reagents used. The higher the concentrations of CEES, Au, O_2, and the lower the concentration of H_2O, the shorter the

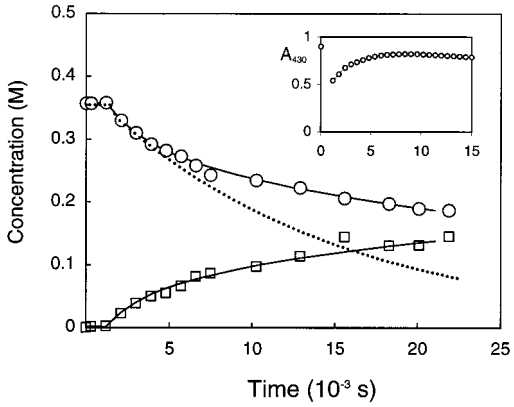

Figure 2. Kinetics of CEES oxidation by the $HAuCl_4/0.75AgNO_3/1.25AgClO_4/O_2$ system. CEES consumption and CEESO formation as a function of time are indicated by the symbols ○ and □, respectively. Inset: absorbance at 430 nm as a function of time (the absorbance remains constant after 15 000 s, ∼4 h). Solid lines represent a fitting of CEES consumption and CEESO formation to the theoretical model in the text. The theoretical kinetic curve (simple-exponential decay with pseudo-first-order rate constant; $k_{obs} = 7 \times 10^{-5}$ s^{-1}) for CEES consumption, assuming no inhibition by CEESO is indicated by the dotted line. Conditions: 25 °C; 1 atm O_2; $[HAuCl_4] = 4.8$ mM; $[AgNO_3] = 3.6$ mM; $[AgClO_4] = 6.0$ mM.

(65) De Filippo, D.; Devillinova, F.; Preti, C. *Inorg. Chim. Acta* **1971**, *5*, 103−108.

(66) Natile, G.; Bordignon, E.; Cattalini, L. *Inorg. Chem.* **1976**, *15*, 246−248.

(67) Weisser, H. B. *Inorganic Colloid Chemistry*; John Wiley & Sons: New York, 1933; Vol. 1, Chapter 3.

(68) Weisser, H. B. *Inorganic Colloid Chemistry*; John Wiley & Sons: New York, 1933; Vol. 1, p 26.

(69) With the exception of $[Au(CN)_2]^-$, Au(I) complexes disproportionate in H_2O and several disproportionation equilibria have been measured: (a) Schmid, G. M.; Curley-Fiorino, M. E. *Encylopedia of Electrochemistry of the Elements*; M. Dekker: New York, 1975; Vol. 4. (b) Skibsted, L. H.; Bjerrum, J. *Acta Chim. Scand., Ser. A* **1977**, *31*, 155−156. (c) Goolsby, D.; Sawyer, D. T. *Anal. Chem.* **1968**, *40*, 1978. (d) Fenske, G. P.; Mason, W. R. *Inorg. Chem.* **1974**, *13*, 1783−1786. Although disproportionation is less favorable kinetically in CH_3CN solution, it is possible that the catalyst inactivates by hydrolysis of the Au(I) intermediate followed by its reduction to form Au(0): Kissner, R.; Welti, G.; Geier, G. *J. Chem. Soc., Dalton Trans.* **1997**, *10*, 1773−1777.

(70) Mason, W. R.; Gray, H. B. *Inorg. Chem.* **1968**, *7*, 7.

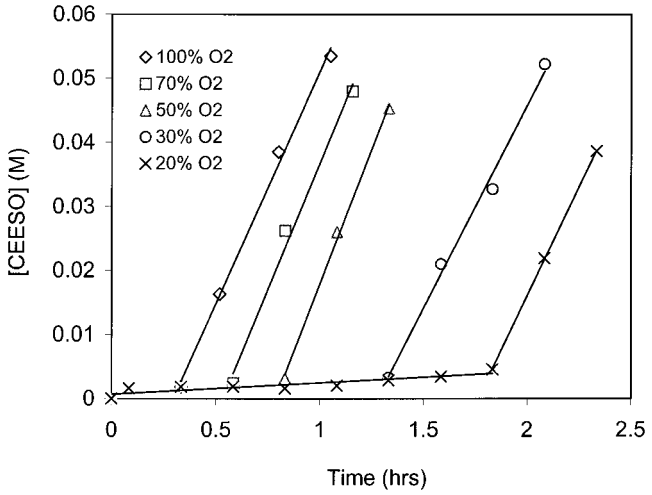

Figure 3. Induction period as a function of initial O_2 concentration in the $HAuCl_4/0.75AgNO_3/1.25AgClO_4/O_2$ system: 100% O_2 = 1.0 atm O_2; 70% O_2 = 0.7 atm O_2; 50% O_2 = 0.5 atm O_2; 30% O_2 = 0.3 atm O_2; 20% O_2 = 0.2 atm O_2. In every case except 100% O_2, the total gas pressure is adjusted to 1 atm using Ar. Conditions: 25 °C; $[HAuCl_4]$ = 4.8 mM; $[AgNO_3]$ = 3.6 mM; $[AgClO_4]$ = 6.0 mM; [CEES] = 0.15 M.

induction period (Figure 3 shows the $[O_2]$ dependence of the induction period).

For clarification of the rate-limiting step in these Au-catalyzed O_2-based oxidations, we sought to determine whether Au(I) and/or Au(III) was the dominant redox state of Au during conditions of catalytic turnover. This was assessed by examining the absorbance for Au(III) after the induction period as a function of the concentration of both CEES and O_2 with all other reactants and conditions kept constant in each case. The quantity of Au(III) was independent of both reactants ([CEES] from 0.05 to 0.37 M and $[O_2]$ from 50 to 100%) within experimental error, and all the Au during turnover was effectively Au(III). Clearly, reduction of Au(III) species and not oxidation of Au(I) species is rate limiting in these aerobic oxidation reactions.

Reaction Stoichiometry. Once the catalyst preparation stoichiometry (eq 1) and the general features of the reaction including the induction period and main reaction were clear, then and only then could the stoichiometry of the main catalyzed reaction be determined clearly. By quantifying O_2 consumption as well as CEES consumption and CEESO formation, the stoichiometry of the reaction was established to be that in eq 2.

$$\mathrm{RSR\ (CEES)} + {}^1/_2\mathrm{O_2} \xrightarrow[\text{catalyst}]{\text{Au-based}} \mathrm{RS(O)R\ (CEESO)} \quad (2)$$

$$\mathrm{SubH_2} + {}^1/_2\mathrm{O_2} \rightarrow \mathrm{Sub} + \mathrm{H_2O} \quad (3)$$

This "dioxygenase" stoichiometry is the optimal one generally sought in air-based oxidations because it is 100% atom efficient (all of the oxidizing capacity of the oxidants and the atoms of the oxidant are accounted for in the desired product). However, other net reactions (stoichiometries) for O_2/air oxidations are also possible, including the general and more common "oxidative dehydrogenation" process (eq 3 for substrate = $SubH_2$). While oxidative dehydrogenations are known in thioether oxidations,[16] clearly this mechanism is more favorable for easily dehydrogenated substrates or those with no oxidizable lone pairs including aliphatic hydrocarbons and alcohols.

Determination of stoichiometry also involves the product selectivity. Sulfoxides, of course, can be and often are oxidized further to the corresponding sulfones. However, in our case, the selectivity for CEESO is very high (97 ± 5%).

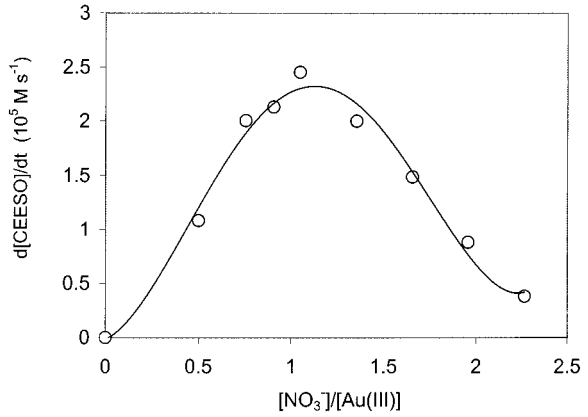

Figure 4. Rate of CEESO formation as a function of $[NO_3^-]/[Au(III)]$. Conditions: 25 °C; 1 atm O_2; $[HAuCl_4]$ = 4.8 mM; [CEES] = 0.37 M.

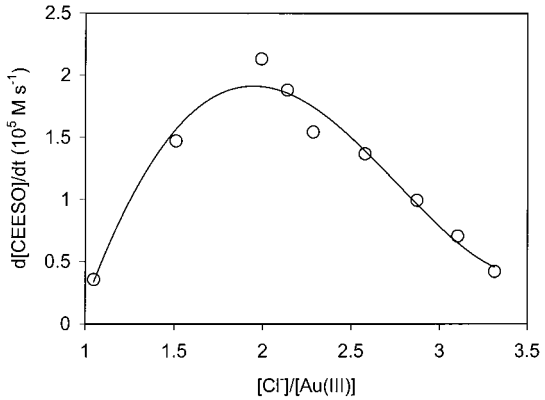

Figure 5. Rate of CEESO formation as a function of $[Cl^-]/[Au(III)]$. Conditions: 25 °C; 1 atm O_2; $[HAuCl_4]$ = 4.8 mM; [CEES] = 0.37 M.

Empirical Rate Law. The rate data are presented here and fully evaluated in context with mechanism elucidation in the Discussion section. The primary experimentally determined rate parameter was +d[CEESO]/d*t*, which is indicated henceforth as "rate", but −d[CEES]/d*t* was also evaluated in many cases. The rate for eq 2 was determined as a function of the concentrations not only of Au(III), Ag(I), CEES, and O_2 but also of NO_3^-, Cl^-, H_2O, $Au/Cl^-/NO_3^-$ together in a constant 1:2:1 mole ratio, and DMSO as a model for the CEESO product. A product model compound is helpful to assess product inhibition because its chemistry can be evaluated independently of the concentrations of all species in the main reaction itself. Determination of the experimental rate law for the reaction was not the usual straightforward process of evaluating the slopes of van′t Hoff ln−ln kinetics plots (ln observed rate versus ln of concentration of varied reactant), because linear plots were not obtained with respect to any reacting species.

Figures 4−8 give, respectively, the dependences of the rate of the main reaction, eq 2, on the concentrations of NO_3^-, Cl^-, CEES, H_2O, and total Au(III) ($Au(III)_T$). For the $Au(III)_T$ dependence, the 1:2:1 ratio of $Au/Cl^-/NO_3^-$ was kept constant. The fittings in Figures 6 and 8 ([CEES] and $[Au(III)_T]$ dependences, respectively) are addressed in the Discussion section. Interestingly, both NO_3^- and Cl^- are critical for reaction, and the dominant transition-state complex appears to contain one NO_3^- and two Cl^- groups. Independently, it was established that replacement of NO_3^- by ClO_4^-, PF_6^-, BPh_4^-,

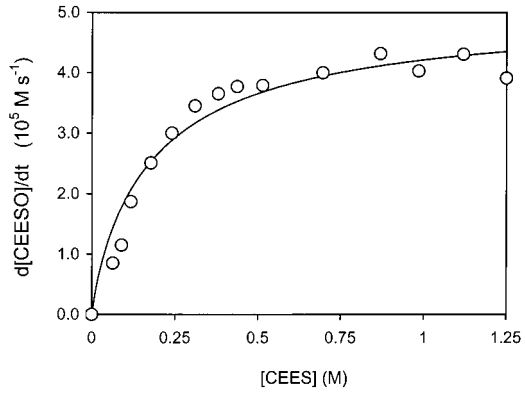

Figure 6. Rate of CEESO formation as a function of initial CEES concentration. The solid curve is a best least-squares fit to eq 19, namely, the bimolecular reaction. Conditions: 25 °C; 1 atm O_2; $[HAuCl_4] = 4.8$ mM; $[AgNO_3] = 3.6$ mM; $[AgClO_4] = 6.0$ mM.

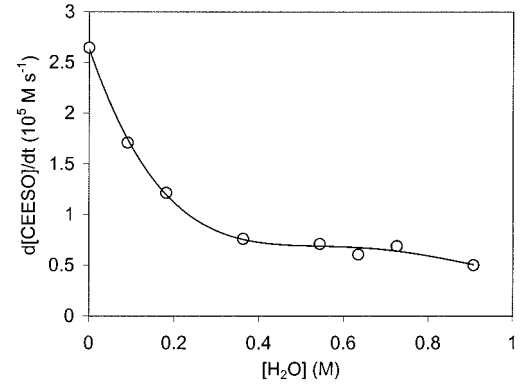

Figure 7. Rate of CEESO formation as a function of H_2O concentration. Conditions: 25 °C; 1 atm O_2; $[HAuCl_4] = 4.8$ mM; $[AgNO_3] = 3.6$ mM; $[AgClO_4] = 6.0$ mM; [CEES] = 0.37 M.

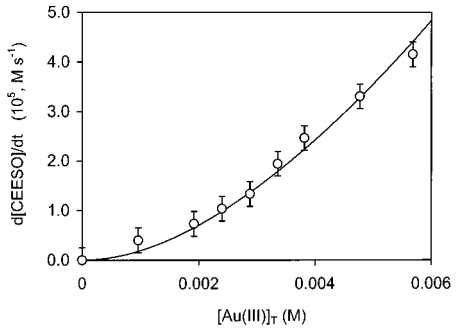

Figure 8. Rate of CEESO formation as a function of the concentration of total catalyst ($Au(III)_T = Au/Cl/NO_3$ in 1:2:1 ratio). The solid curve is a best least-squares fit to eq 19, namely, the bimolecular reaction. Conditions: 25 °C; 1 atm O_2; [CEES] = 0.37 M.

or HSO_4^- generated species with little or no catalytic activity, confirming a significant and specific role for NO_3^- in the active catalyst.

The rate dependence on the concentration of the substrate, CEES, shows saturation kinetics consistent with one or more intermediates in the rate-limiting step(s) containing varying numbers of coordinated CEES molecules. Not surprisingly, the [H_2O] and [DMSO] dependencies (Figure 7 and Table 1, respectively) are hyperbolic (largely inverse), consistent with both H_2O and DMSO competing with Cl^-, NO_3^-, and CEES for open coordination sites on the catalytic Au center and thus decreasing the concentration of the Au complexes required for CEESO production.

Table 1. Rate of CEESO Formation as a Function of [DMSO][a]

[DMSO], M	0	0.022	0.029	0.036	0.043	0.072	0.14	0.22	0.36
rate × 10^5, M s^{-1}	2.9	1.84	1.40	1.33	1.01	0.69	0.49	0.42	0.24

[a] Conditions: 25 °C; 1 atm O_2; $[HAuCl_4] = 4.8$ mM; $[AgNO_3] = 3.6$ mM; $[AgClO_4] = 6.0$ mM; [CEES] = 0.37 M.

The rate is independent of O_2 concentration. This is consistent with the Au oxidation state during turnover (vide supra) and implicates that Au(III) reduction and not Au(I) reoxidation is rate limiting. Interestingly, in the one other documented case of thioether oxidation catalyzed by soluble Au complexes, the oxidation of thioethers to sulfoxides by HNO_3 reported by Gasparrini et al., the rate-limiting step is reoxidation of Au(I) to Au(III).[37]

One experiment to assess the mechanism of the slow thioether oxidation−Au(III) reduction step involved evaluation of the overall reaction rate when Cl^- was replaced by Br^- under otherwise identical conditions. At 0.3 M CEES, the initial rates for CEESO production for the Cl^--containing and Br^--containing systems are 2.0×10^{-5} and 3.4×10^{-5} M s^{-1}, respectively. At 3.0 M CEES, these initial rates are 3.9×10^{-5} and 7.3×10^{-5} M s^{-1}, respectively. These and other results clarify the nature of this step (see Discussion section).

The temperature dependence (activation parameters) of the reaction was purposefully not assessed because reactions with several preequilibrium steps, such as the one in this study (see Discussion section), would yield minimally interpretable, and possibly misleading data.

H_2O_2 can oxidize CEES to CEESO in CH_3CN, when a strong acid is present. Furthermore, HCl from catalyst generation, eq 1, and the reactant $HAuCl_4$ itself are acidic. Since H_2O_2 could be formed in situ during Au(I) reoxidation by O_2, we assessed the possibility of CEES oxidation by intermediate H_2O_2 using an isotope labeling study. A reaction with $H_2{}^{18}O$ in place of regular $H_2{}^{16}O$ was conducted to provide this information and also to ascertain whether the oxygen in the product sulfoxide, CEESO, derives from H_2O, H_2O_2, or O_2. The CEESO produced in the early part of the reaction (up to 10 turnovers) is ∼80% ^{18}O and ∼20% ^{16}O. The somewhat lower percent ^{18}O in the CEESO than in the $H_2{}^{18}O$ used derives in part from water molecules associated with $HAuCl_4$, a hygroscopic compound that is hard to dry. The percentage of ^{18}O in the CEESO decreases with reaction time and turnovers. After 60 turnovers, the ^{18}O in the CEESO decreases to ∼60 atom %. These data indicate that CEESO is produced by a process involving only H_2O and not O_2 or H_2O_2. If H_2O_2 alone were involved, the $^{18}O/^{16}O$ ratio would not exceed 50%. The time dependence of the label is consistent with a consumption of labeled water which results in a dilution of the $H_2{}^{18}O$ pool with $H_2{}^{16}O$ (while no net H_2O is formed in the overall reaction, eq 2, H_2O is consumed and then regenerated in the mechanism, vide infra).

The rates of CEESO production, eq 2, in both 100% H_2O (usual conditions) and in ∼100% D_2O were determined. The rates were the same within the experimental error (±5%).

Discussion

A mechanism for the selective aerobic oxidation of thioethers to sulfoxides catalyzed by Au(III) complexes that is compatible with all the data and the literature investigations (stoichiometric thioether−Au(III) reactions) is given in Scheme 1. While NO_3^- is capable of reoxidizing the product Au(I) back to Au(III) as demonstrated by Natile and co-workers,[37] *O_2 and not NO_3^- is the terminal oxidant in our system*. This is established because

Scheme 1. Mechanism for O_2-Based Oxidation of Thioethers Catalyzed by $Au(III)Cl_2NO_3$ (thioether) (**1**)

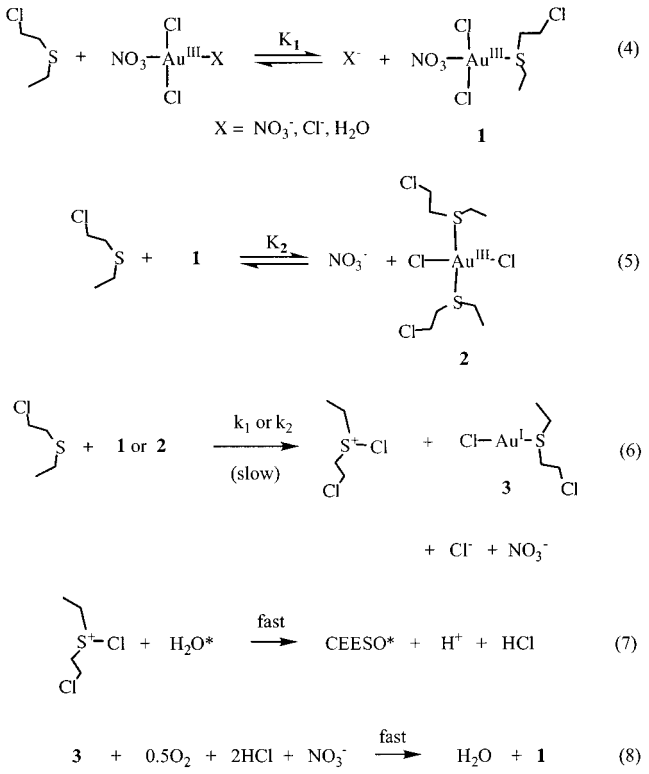

there is only 1 equiv of NO_3^- in our reactions, yet most of them have been taken to 30 or more turnovers and in one case 200 turnovers (200 equiv of CEESO product per equivalent of Au and equivalent of NO_3^-). Figures 4 and 5 indicate that the kinetically dominant species leading to CEESO contains Au, Cl^-, and NO_3^- in a 1:2:1 ratio, and Figure 6 indicates that this species also contains CEES (Figure 6 is addressed further below). Dimeric or oligomeric d^8 square-planar Au(III) are not particularly common,[30] and a monomeric Au(III) complex with two Cl^- ligands, one NO_3^- ligand, and at least one CEES ligand is likely. While 5-coordinate Au(III) complexes cannot be rigorously ruled out, they are not likely to be significant.[71] All the information on oxidation of thioethers by Au(III) complexes is consistent with the rapid exchange of all ligands on Au(III) prior to thioether oxidation.[32−36] For the present catalytic system, these preequilibria are summarized by eqs 4 and 5 in Scheme 1. Explicitly, Cl^-, NO_3^-, and CEES lead to formation of the Au(III) complexes required for CEESO formation: a complex with one CEES ligand (henceforth **1**), with formation constant K_1, and a complex with two CEES ligands (henceforth **2**), with formation constant K_2. These ligands drive eq 4 to the right. H_2O (data in Figure 7), and the CEESO product, modeled by another sulfoxide, DMSO (data in Table 1), both inhibit the rate of reaction by decreasing the concentrations of the Au(III) complexes required for CEESO formation. These ligands drive eq 4 to the left. For completeness, CH_3CN may also competitively bind to Au(III), but this cannot be assessed since it is the solvent.

(71) The only 5-coordinate Au(III) complexes with appreciable stability contain chelating ligands such as bromodicyano(1,10-phenanthroline)-gold(III) isolated from dimethylformamide: Marangoni, G.; Pitteri, B.; Bertolasi, Y.; Gilli, G.; Ferretti, V. *J. Chem. Soc., Dalton Trans.* **1986**, 1941. If there is an interaction between a positive Au(III) center and a negative axial ligand counterion, this ligand would likely be Cl^-, because NO_3^- associates very weakly with Au(III) (and not at all with Au(I).

Literature studies of thioether-Au(III) reactions establish that Au(III) complexes with one thioether ligand, such as **1**, are considerably more abundant in solutions of excess thioether than complexes with two thioether ligands, such as **2** ($K_1 \gg K_2$).[35,36] No Au(III) complex with three thioether ligands is given in Scheme 1 because there are no data indicating these species form in measurable quantities (i.e., $K_2 \gg K_3$; $K_3 \sim 0$). Evaluation of the kinetics data below also indicates that **1** and not **2** is the kinetically dominant Au(III) complex for catalytic aerobic oxidation of CEES to CEESO.

Three lines of evidence establish that the redox step, oxidation of thioether/reduction of Au(III), eq 6 in Scheme 1, is rate limiting in the catalytic O_2-based oxidation of thioethers: First, all the rate information (Figures 4−8) are consistent with this; second, the rate is independent of O_2 pressure, and third, Au(III), not Au(I), is the dominant form of Au during catalytic turnover. The rate constants k_1 and k_2 in eq 6 are for **1** and **2**, respectively; however, eq 6 has been written in terms of **1** and its redox products, $(CEES)Au^ICl$ (**3**), Cl^-, and NO_3^- (versus **2** and its products), because most of the observed chemistry derives from **1**. Because eq 6 is clearly rate determining, the subsequent steps, eqs 7 and 8, are not.

There are several possible mechanisms for the rate-limiting redox step, eq 6, but one is more consistent with the data, analysis of the data below, and the stoichiometric Au(III)−thioether studies in the literature. First, a mechanism involving rate-limiting formation of the required Au(III) complex (primarily **1** in our case) prior to redox chemistry is not compatible with any of the literature studies, nor is it compatible with the kinetic requirement of two molecules of thioether in the slow step. The detailed equilibrium and kinetics studies (extensive data and fitting) of two groups establish that two molecules of thioether are involved in the slow step: Natile and co-workers[36] on the oxidation of a Me_2S, Et_2S, and *n*-Pr_2S by $Au(III)(Cl)_x(RS)_{4-x}$ and Elding and co-workers[35] on the oxidation of a Me_2S by *trans*-$Au(III)(CN)_2(Cl)_{2-x}(RS)_{2-x}$. While the Natile system and ours differ in three ways, theirs does not undergo catalytic turnover, does not contain NO_3^-, and is in 95:5 CH_3OH/H_2O (versus CH_3CN in our case), the Au(III)−thioether coordination and redox chemistry in the two systems are otherwise very similar. Elding's complex, while not as close to ours as that of Natile, nonetheless shares structural and redox chemistry very similar to ours as well.

A second possible mechanism is an intramolecular decomposition of the required Au(III) complex, eqs 9 and 10.

$$\mathbf{1} \xrightarrow{k_{\text{intra}}^1} Cl{-}Au^I{-}CH_3CN + CEES^+{-}Cl + NO_3^- \quad (9)$$

$$\mathbf{2} \xrightarrow{k_{\text{intra}}^2} Cl{-}Au^I{-}CEES + CEES^+{-}Cl \quad (10)$$

This is effectively a rate-limiting reductive elimination to form a thioxonium salt (whose fate, eq 7 in Scheme 1, is addressed below) and a Au(I) complex. While this mechanism has been proposed for some thioether oxidations by Au(III),[32,34,35] it is likely not operable in our catalytic aerobic oxidation chemistry. First, eq 9 is not compatible with the finding that two molecules of thioether are involved in the rate-limiting redox step (vide supra).[35,36] However, this argument does not eliminate eq 10, which involves two thioether molecules. The conversion of **2** to **3** + CEESO can, in principle, be assisted by H_2O, eq 11,[35]

$$\mathbf{2} \xrightarrow[H_2O]{} Cl{-}Au^I{-}CEES + CEESO + HCl \quad (11)$$

but the nonexistent solvent effect ($k_{H_2O}/k_{D_2O} = 1.0$) argues against eq 11 being rate limiting. Again, the kinetics data are in accord with H_2O functioning as an inhibitor via competition for the pool of Au(III) complexes present during catalytic turnover, i.e., driving eq 4, Scheme 1, to the left.

Additional evidence against the unimolecular collapse of **1** and **2** (eqs 9 and 10) derives from analysis of the reaction kinetics, which we now address. If eqs 9 and 10 were rate limiting, the overall rate would be eq 12. It is reasonable to

$$\text{rate} = k^1_{\text{intra}}[\mathbf{1}] + k^2_{\text{intra}}[\mathbf{2}] \quad (12)$$

assume, that under our experimental conditions, $[AuCl_2NO_3(CH_3CN)] \ll [\mathbf{1}] + [\mathbf{2}]$, since K_1 is big and $[CEES] \gg [Cl^-] + [NO_3^-]$. The equilibrium expressions from eqs 4 and 5, Scheme 1, and reaction mass balance expressions afford eqs 13 and 14, from which we can write eqs 15 and 16. Expressions for [**1**] and [**2**], eqs 17 and 18, are obtained by

$$K_2[\mathbf{1}][CEES] = [\mathbf{2}][NO_3^-] = [\mathbf{2}]^2 \quad (\text{because } [\mathbf{2}] = [NO_3^-]) \quad (13)$$

$$[\mathbf{1}] + [\mathbf{2}] = [Au(III)]_T \quad (\text{since } [Au(I)] \ll [Au(III)]) \quad (14)$$

$$[\mathbf{2}] = (K_2[\mathbf{1}][CEES])^{0.5} \quad (15)$$

$$[\mathbf{1}] + (K_2[\mathbf{1}][CEES])^{0.5} = [Au(III)]_T \quad (16)$$

solving eqs 15 and 16:

$$[\mathbf{1}] = (1/4)(\sqrt{K_2[CEES] + 4[Au(III)]_T} - \sqrt{K_2[CEES]})^2 \quad (17)$$

$$[\mathbf{2}] = [Au(III)]_T - (1/4)(\sqrt{K_2[CEES] + 4[Au(III)]_T} - \sqrt{K_2[CEES]})^2 \quad (18)$$

Combining eqs 12, 17, and 18 gives eqs 19a and 19b for the reaction rate.

$$\text{rate} = k^2_{\text{intra}}[Au(III)]_T + (k^1_{\text{intra}} - k^2_{\text{intra}})[\mathbf{1}] \quad (19a)$$

$$\text{rate} = k^2_{\text{intra}}[Au(III)]_T + (1/4)(k^1_{\text{intra}} - k^2_{\text{intra}}) \times (\sqrt{K_2[CEES] + 4[Au(III)]_T} - \sqrt{K_2[CEES]})^2 \quad (19b)$$

This rate law indicates that reaction rate orders depend on whether **1** or **2** is more reactive. If $k^1_{\text{intra}} > k^2_{\text{intra}}$, then the rate will increase quadratically with $[AuIII)]_T$, but will decrease with [CEES]. On the contrary, if $k^1_{\text{intra}} < k^2_{\text{intra}}$, then the rate will increase with both $[AuIII)]_T$ and [CEES], finally reaching saturation with an observed reaction rate order of <1. Thus, one of the rate dependences, either that for [CEES] or that for $[AuIII)]_T$, can be easily fitted, but not both simultaneously. Importantly, however, the experimental data (Figures 6 and 8) are incompatible with either of these scenarios based on the unimolecular collapse mechanism (eqs 9 and 10), which further rules out this mechanism. In addition, the water-assisted collapse, eq 11, is kinetically the same as eq 10, and incorporation of eq 11 in the above analysis leads to an expression analogous to eq 19 but with k^2_{intra} replaced by $k^{2/\text{obs}}_{\text{intra}} = \{k^2_{\text{intra}}$ (reaction 10) + k^2_{intra} (reaction 11)$\}$. Thus, eq 11 is also incompatible with the data and can also be ruled out as a mechanism.

A third mechanism involving rate-limiting CEES attack at the Au(III) center with immediate fast CEES oxidation and Au(III) reduction is very unlikely. This S_N2-like mechanism does not appear to be operable in any of published stoichiometric Au(III)−thioether systems, nor is it compatible with the relative rates of oxidation of Me_2S, Et_2S, and *n*-Pr_2S by $Au(III)(Cl)_x(R_2S)_{4-x}$ reported by the Italian group.[36] These rates were sensitive to the basicity but not sensitive to the steric bulk of the thioether: Me_2S (slowest) < Et_2S < *n*-Pr_2S (fastest), the opposite trend observed in S_N2-like processes.

A fourth possible mechanism involves bimolecular attack of thioether on a coordinated ligand of Au(III). This is the proposed mechanism for some but not all of the stoichiometric thioether oxidations by Au(III).[31−33] None of the data on our system rules this out, and it is consistent with the increase in rate when Cl^- is replaced by Br^- under otherwise identical conditions. Ligand transfer oxidation processes, including reduction of Au(III) by thioether in our case, are kinetically favored by soft Br^- (versus harder Cl^-) ligands.[72] This kinetic preference for softer ligands is in the direction opposite from the thermodynamics of the reaction. Specifically, the metal centers with Br^- in place of Cl^- at parity of other ligands have lower potentials and are weaker oxidants. Additional evidence comes indirectly from the following analysis of our kinetic data.

The overall rate from Scheme 1 and eq 14 is eq 20.

$$\text{rate} = k_1[\mathbf{1}][CEES] + k_2[\mathbf{2}][CEES] = k_1[CEES][Au(III)]_T + (k_1 - k_2)[CEES][\mathbf{1}] \quad (20)$$

Combining eqs 17 and 20 gives eqs 21a and 21b for the reation rate

$$\text{rate} = k_2[CEES][Au(III)]_T + (k_1 - k_2)[CEES][\mathbf{1}] \quad (21a)$$

$$\text{rate} = k_2[CEES][Au(III)]_T + ((k_1 - k_2)[CEES]/4)(\sqrt{K_2[CEES] + 4[Au(III)]_T} - \sqrt{K_2[CEES]})^2 \quad (21b)$$

The best fitting of the experimental data (solid curve in Figure 6) gives $k_1 = 0.12 \pm 0.05\ M^{-1}s^{-1}$, $K_2 = 0.04 \pm 0.02$, and $k_2 = 0$. The errors were estimated at the 95% confidence limit. In other words, since $k_2 = 0$, eq 21 simplifies to eq 22.

$$\text{rate} = (k_1[CEES]/4)(\sqrt{K_2[CEES] + 4[Au(III)]_T} - \sqrt{K_2[CEES]})^2 \quad (22)$$

A low reactivity of complex **2** toward CEES, $k_2 = 0$, is easily demonstrated without curve fitting. At high [CEES], the majority of Au(III) is present as **2**, which corresponds to $K_2[CEES] \gg 4[Au(III)]_T$. Multiplying eq 17 by the unity factor ($K_2[CEES]/K_2[CEES]$) affords eq 23.

$$[\mathbf{1}] = (K_2[CEES]/4)(\sqrt{1 + 4x} - 1)^2 \approx (K_2[CEES]/4) \times \{(1 + 2x) - 1\}^2 = [Au(III)]_T^2/K_2[CEES] \quad (23)$$

where $x = [Au(III)]_T/K_2[CEES] \ll 1$.

(72) Kochi, J. K. In *Oxidation−Reduction Reactions of Free Radicals and Metal Complexes*; Kochi, J. K., Ed.; Wiley: New York, 1973; Vol. 1, pp 591−685.

Equation 18 then simplifies to eq 24, and the rate law is then eq 25.

$$[\mathbf{2}] = [\mathrm{Au(III)}]_T - [\mathbf{1}] \approx [\mathrm{Au(III)}]_T/(1 - [\mathrm{Au(III)}]_T/K_2[\mathrm{CEES}]) \quad (24)$$

$$\text{rate} = (k_1 - k_2)[\mathrm{Au(III)}]_T^2/K_2 + k_2[\mathrm{CEES}][\mathrm{Au(III)}]_T \quad (25)$$

Equation 25 predicts that the reaction should be first order with respect to CEES at high [CEES] with the slope of $k_2[\mathrm{Au(III)}]_T$. However, Figure 6 indicates the rate increases linearly at low [CEES] and approaches saturation at [CEES] > 0.4 M. This saturation kinetics in [CEES] clearly suggests that $k_2 = 0$. The data and fitting state that, at high [CEES], the CEES substrate itself slows the reaction by favoring formation of the less reactive **2** by displacing NO_3^- and/or Cl^- from the more reactive **1**.

In addition, the dependence of the rate on $[\mathrm{Au(III)}]_T$ was fit by eq 22. The result is the solid curve in Figure 8 with $k_1 = 0.11\ M^{-1}\ s^{-1}$, $K_2 = 0.05$, and $k_2 = 0$ (vide supra). However, this fit is not as reliable as the fit of the rate versus [CEES] data (Figure 6). Several local minimums and high experimental errors at low $[\mathrm{Au(III)}]_T$ result in large errors (a factor of ~3 at the 95% confidence limit) for k_1 and K_2. Nonetheless, these values are in good agreement with those obtained from the fit of the rate versus [CEES] data ($k_1 = 0.12 \pm 0.05\ M^{-1}\ s^{-1}$ and $K_2 = 0.04 \pm 0.02$). Our value for K_2 is very similar to that found by Natile and co-workers for complexation of Me_2S to $AuCl_4^-$: $K_2 = 0.08 \pm 0.02$.[36] However, their system gave $k_2/k_1 \sim 12$.[36] While the two systems are very similar, theirs does not contain NO_3^- and is in 5% aqueous methanol (versus CH_3CN in our case). In addition, H_2O accelerates their reaction, but it inhibits ours.[36]

The process in the mechanism after the slow step involves conversion of the oxidized sulfur center to the sulfoxide. The necessary initial product of this process is a chlorosulfonium ion (eq 7, Scheme 1). These species are precedented, and they are known to hydrolyze rapidly to give sulfoxides.[73] The isotope labeling study is completely consistent with this mechanism, namely, that the source of oxygen in the sulfoxide is H_2O, not O_2. Note that although the stoichiometry is that of oxygenation, eq 2, the mechanism involves consumption of water, eq 7, and its subsequent regeneration, eq 8.

Finally, as stated in the Results section, the reaction slows down with time, a likely reflection of self-inhibition (i.e., inhibition by products in this instance). DMSO, a molecule structurally and electronically similar to the CEESO product, was used to probe inhibition by sulfoxides. The fast exchange of the Au(III) ligands (facile preequilibria) should include sulfoxide as it forms, and thus sulfoxide should compete with NO_3^- and/or Cl^- present in **1** to form less active complexes **2′** and **2″** (the analogues of **2**, but with DMSO or CEESO as ligands in place of CEES, respectively), eqs 26 and 27. Because the concentration of **1** decreases, the reaction slows down. This is what is observed experimentally: DMSO at concentrations of >14 mM decreases the reaction rate (Table 1). A full evaluation of the DMSO inhibition data and the kinetics of self-inhibition by CEESO (hyperbolic association functions, nonlinear fitting, etc.) are given in Appendix 1. These analyses lead to the following equilibrium constant values: $K_2^{\mathrm{DMSO}} = 12$ and $K_2^{\mathrm{CEESO}} = 23$. Finally, Figure 2 gives the observed kinetics of CEES oxidation and CEESO formation (data points), the theoretical fits of each (solid lines), and the anticipated CEES consumption if there were no inhibition by CEESO (dotted line).

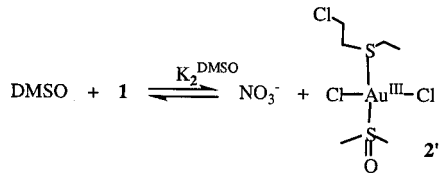

(26)

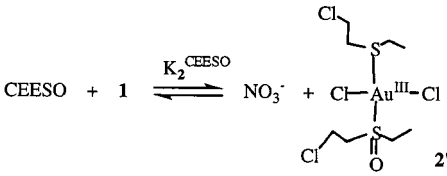

(27)

Conclusions

(1) While neither $HAuCl_4$ or $AgNO_3$ catalyzes aerobic sulfoxidation (O_2 or air oxidation of thioethers to sulfoxides), these compounds, when mixed in CH_3CN, form $\mathrm{Au(III)Cl_2NO_3(thioether)}$ (**1**), an extremely active catalyst for this type of reaction. Thioethers are oxygenated using only O_2 as a terminal oxidant at rates that are orders of magnitude larger than those exhibited by the fastest existing catalysts, $Ru(DMSO)_4Cl_2$ and $(NH_4)_2Ce(NO_3)_6$.

(2) The association equilibria represented by eqs 4 and 5 (Scheme 1) account for the affects on the rate of CEESO production of nearly all species present: H_2O inhibits by driving eq 4 unproductively to the left; CEES inhibits at high [CEES] by driving eq 5 unproductively to the right; PF_6^-, BPh_4^-, and HSO_4^- do not affect the rate because K_1 in Scheme 1 is too small for these species to be kinetically significant; and the CEESO product inhibits by competing for coordination positions on **1**, the productive Au(III) complex, in equilibria analogous to eq 4.

(3) The general rate law, the independence of rate on O_2 pressure/concentration, and the dominance of Au(III) versus Au(I) under turnover conditions collectively establish that Au(III) reduction by thioether substrate is rate limiting.

(4) The rate-limiting step involves bimolecular attack of thioether (CEES) on the chloride ligand of Au(III). The most active complex, **1**, contains one CEES, one nitrate, and two chloride ligands.

(5) The reaction is modestly inhibited by sulfoxide product because sulfoxide competes with CEES substrate for Au(III).

Acknowledgment. We thank the U.S. Army Research Office for support of this research. We thank Dr. Ira A. Weinstock for discussion and helpful comments.

Supporting Information Available: List of the 150 catalysts represented in the library (Figure 1). This material is available free of charge via the Internet at http://pubs.acs.org.

Appendix 1 (Inhibition by Sulfoxide)

Equation 26 yields eq 28, reaction mass balance yields eq 29, and eqs 13 and 28 yield eq 38.

$$K_2^{\mathrm{DMSO}}[\mathbf{1}][\mathrm{DMSO}] = [\mathbf{2'}][NO_3^-] \quad (28)$$

$$[\mathbf{1}] + [\mathbf{2}] + [\mathbf{2'}] = [\mathrm{Au(III)}]_T \quad (\text{since } [\mathrm{Au(I)}] \ll [\mathrm{Au(III)}]) \quad (29)$$

$$(K_2^{\mathrm{DMSO}}[\mathrm{DMSO}] + K_2[\mathrm{CEES}])[\mathbf{1}] = ([\mathbf{2}] + [\mathbf{2'}])[NO_3^-] = ([\mathbf{2}] + [\mathbf{2'}])^2 \quad (\text{since } [NO_3^-] = [\mathbf{2}] + [\mathbf{2'}]) \quad (30)$$

(73) Smith, S. G.; Winstein, S. *Tetrahedron* **1958**, *3*, 317.

Equations 29 and 30 afford eq 31, an expression for [**1**], which is analogous to eq 17 but contains, in addition, DMSO.

$$[\mathbf{1}] + (1/4)(\sqrt{K_2[\mathrm{CEES}] + K_2^{\mathrm{DMSO}} + 4[\mathrm{Au(III)}]_\mathrm{T}} - \sqrt{K_2[\mathrm{CEES}] + K_2^{\mathrm{DMSO}}\,[\mathrm{DMSO}]})^2 \quad (31)$$

At high [CEES] and DMSO, the majority of Au(III) is present mainly **2** and **2′**, which corresponds to $K_2[\mathrm{CEES}] + K_2^{\mathrm{DMSO}}[\mathrm{DMSO}] \gg 4[\mathrm{Au(III)}]_\mathrm{T}$. Equation 31 then simplifies to eq 32 (for details, see eq 23), which then gives the rate law in eq 33.

$$[\mathbf{1}] \approx [\mathrm{Au(III)}]_\mathrm{T}^2/(K_2[\mathrm{CEES}] + K_2^{\mathrm{DMSO}}[\mathrm{DMSO}]) \quad (32)$$

$$\mathrm{rate} = k_1[\mathbf{1}][\mathrm{CEES}] \approx k_1[\mathrm{CEES}][\mathrm{Au(III)}]_\mathrm{T}^2/(K_2[\mathrm{CEES}] + K_2^{\mathrm{DMSO}}[\mathrm{DMSO}]) = (k_1/K_2)[\mathrm{Au(III)}]_\mathrm{T}^2/(1 + K_2^{\mathrm{DMSO}}[\mathrm{DMSO}]/K_2[\mathrm{CEES}]) = r_\mathrm{o}/(1 + K_2^{\mathrm{DMSO}}[\mathrm{DMSO}]/K_2[\mathrm{CEES}]) \quad (33)$$

where $r_\mathrm{o} = (k_1/K_2)[\mathrm{Au(III)}]_\mathrm{T}^2$ is the initial rate in the absence of DMSO (for comparison, see eq 25). Thus, under certain experimental conditions, when $K_2[\mathrm{CEES}] + K_2^{\mathrm{DMSO}}[\mathrm{DMSO}] \gg 4[\mathrm{Au(III)}]_\mathrm{T}$), the dependence of the reaction rate on [DMSO] is described by a simple hyperbolic function, eq 33. Indeed, the experimental data (Table 1) fitted to eq 33 yield $K_2^{\mathrm{DMSO}} = 12$.

CEESO is likely to inhibit the reaction by the same mechanism as DMSO, eq 28. At [CEES] < 0.4 M, the dependence of reaction rate on [CEES] can be roughly approximated by a linear function $r_\mathrm{o} \approx k_\mathrm{obs}[\mathrm{CEES}]$ (Figure 6). Taking this and mass balance ($[\mathrm{CEESO}] = [\mathrm{CEES}]_\mathrm{o} - [\mathrm{CEES}]$) into account, the rate law is then eq 34, where $[\mathrm{CEES}]_\mathrm{o}$ is the initial CEES concentration. Rearranging eq 34 gives eq 35.

$$\mathrm{rate} = -\mathrm{d}[\mathrm{CEES}]/\mathrm{d}t = -k_\mathrm{obs}[\mathrm{CEES}]/\{1 + K_2^{\mathrm{CEESO}}([\mathrm{CEES}]_\mathrm{o} - [\mathrm{CEES}])/[\mathrm{CEES}]\} \quad (34)$$

$$(\mathrm{d}[\mathrm{CEES}]/[\mathrm{CEES}])\{1 - K_2^{\mathrm{CEESO}} + K_2^{\mathrm{CEESO}}[\mathrm{CEES}]_\mathrm{o}/[\mathrm{CEES}]\} = -k_\mathrm{obs}\,\mathrm{d}t \quad (35)$$

Since at initial time $[\mathrm{CEES}] = [\mathrm{CEES}]_\mathrm{o}$, the integration (a standard integral) gives eq 36:

$$t = (k_\mathrm{obs}{}^{-1})\{(1 - K_2^{\mathrm{CEESO}})\ln([\mathrm{CEES}]_\mathrm{o}/[\mathrm{CEES}]) + K_2^{\mathrm{CEESO}}([\mathrm{CEES}]_\mathrm{o}/[\mathrm{CEES}] - 1)\} \quad (36)$$

The value $k_\mathrm{obs} = 7 \times 10^{-5}\ \mathrm{s}^{-1}$ was determined independently from the slope of the plot of initial reaction rate versus $[\mathrm{CEES}]_0$ at [CEES] < 0.4 M. The difference between experimental time (after the induction period) and that calculated from eq 36 was minimized by varying K_2^{CEESO}. The solid line in Figure 2 is the result of nonlinear least-squares fitting. The dashed line represents the expected consumption of CEES, assuming that no inhibition by CEESO takes place, and the reaction is first order in [CEES] (an exponential decay with $k_\mathrm{obs} = 7 \times 10^{-5}\ \mathrm{s}^{-1}$).

The kinetics of CEESO accumulation (solid line plotted through CEESO kinetics experimental points) was not fitted but calculated from eq 37, where the factor of 0.8 accounts for CEESO decomposition in the hot GC injection port.

$$[\mathrm{CEESO}] = 0.8([\mathrm{CEES}]_\mathrm{o} - [\mathrm{CEES}]) \quad (37)$$

JA0033133